Assessing the textural defect of pastiness in dry-cured pork ham using chemical, microstructural, textural and ultrasonic analyses

M. Contreras[1], J. Benedito[1], A. Quiles[1], J.M. Lorenzo[2], E. Fulladosa[3], P. Gou[3], J.V. Garcia-Perez[1]*

[1]UPV, Universitat Politècnica de València. Departamento de Tecnología de Alimentos. Camí de Vera, s/n, 46022, Valencia, Spain.

[2]CTC, Centro Tecnológico de la Carne de Galicia. Avenida de Galicia 4, Parque Tecnolóxico de Galicia, 32900, San Cibrao das Viñas, Ourense, Spain.

[3]IRTA, XaRTA, Food Technology, Finca Camps i Armet, E-17121 Monells, Girona, Spain.

*Corresponding author: Tel.: +34 963879376; fax: +34 963879839. E-mail address: jogarpe4@tal.upv.es (J.V. Garcia-Perez).

Abstract

The dry-cured pork ham industry lacks non-destructive quality control techniques able to characterize relevant textural defects, such as pastiness or softness. The aim of this study is to analyze the feasibility of using different destructive and non-destructive techniques to characterize pastiness in dry-cured ham. Dry-cured ham processing was modified in order to induce different pastiness intensities over a wide range of moisture and salt contents. Afterwards, pastiness was assessed by sensory analysis and samples classified as non-pasty, medium-pasty and highly-pasty. Finally, chemical, textural, microstructural (LM and TEM) and ultrasonic analyses (velocity and attenuation coefficient) were carried out.

Samples with a high degree of pastiness experienced an increase of 16.8% and 16.7% as regards the proteolysis index and relaxation capacity, respectively, and a 67.7% decrease in hardness compared to non-pasty hams. The microstructural analysis revealed that pastiness brought about great structural degradation. Ultrasonic velocity was significantly related to the salt (r=0.79) and moisture contents (r=0.69), but no influence of pastiness was found on the velocity. However, the attenuation coefficient increased as the pastiness rose and could be considered as a useful parameter for characterizing this complex textural defect. Therefore, ultrasound could be used not only to carry out a non-destructive characterization of dry-cured ham composition but also to assess pastiness.

Keywords; Dry-cured ham, pastiness, texture, microstructure, ultrasound.

1. Introduction

Currently, consumer trend is focusing on reducing the intake of salt in our diets. As one means of reaching this objective, and taking into account that processed meat products constitute one of the major sources of sodium chloride in the diet (Desmond, 2006), dry-cured ham manufacturers are trying to reduce the salt content, while preserving the quality of the final product. Notwithstanding this, salt reduction during processing leads to an excessive proteolytic activity (Parolari et al., 1994; Virgili et al., 1995), resulting in soft, pasty textures (pastiness). Moreover, inherent properties linked to the raw material, such as pH or high water content, have also been identified as factors influencing pastiness, which underlines the complexity of avoiding its incidence and intensity during industrial processing (Morales, Serra, Guerrero, & Gou, 2007). Specifically, pastiness in dry-cured ham is defined as the loss of elasticity in the muscle and, in sensory terms, as a mouth-coating sensation during mastication. The texture of dry-cured ham is one of its most highly-appreciated attributes and notably influences consumer acceptability (Morales et al., 2007a), which highlights the need for its adequate characterization.

Previous literature has already made some attempts to deal with the assessment of pastiness. Thus, Morales, Guerrero, et al. (2007) evaluated the feasibility of two different instrumental texture tests (TPA and stress relaxation) to discriminate between defective and non-defective ham slices, assessing the impact of the assay conditions (temperature and compression crosshead speed) on the characterization results. Likewise, sensory analysis, some chemical properties (pH, salt, moisture, non-protein nitrogen, etc.), proteomic profile and volatile compounds of defective dry-cured ham have also been considered for the characterization of pastiness (Garcia-Garrido et al., 1999; López-Pedrouso et al., 2018; Pérez-Santaescolástica et al., 2018). However, existing literature reveals the need for a deeper understanding and characterization of pastiness. Previous studies lack a significant number of samples studied over a wide range of pastiness levels. In addition, the fact that commercial hams have mostly been

used, indicates that these studies are influenced by the interference of the salt content in the appearance and intensity of pastiness. Moreover, to the best of our knowledge, there has been no previous analysis of pasty ham microstructure, which could provide interesting information with which to understand the changes that take place in this type of texturally defective product.

Sensory, chemical and textural analyses are laborious, relatively slow and destructive. More rapid and non-invasive technologies have been tested to assess pastiness in dry-cured ham. Thus, laser-light backscattering has been used in commercial, sliced dry-cured ham to determine proteolysis, which is a parameter related to the textural characteristics of the product (Fulladosa et al., 2017). However, they found that the scattering area was similar for every level of proteolysis. Additionally, Fulladosa et al. (2018) studied the feasibility of multi energy X-ray to detect changes in dry-cured ham slices after inducing proteolysis, finding a limitation when discriminating between levels of proteolysis because of the interference of the salt and water contents on the X-ray attenuation. As an alternative, low intensity ultrasound could be considered a feasible technology for the purposes of characterizing food composition and texture in a non-destructive way (Benedito, Carcel, Sanjuan, & Mulet, 2000; Corona, García-Pérez, Ventanas, & Benedito, 2014). The automated, cost-effective, non-destructive and minimally invasive characteristics of ultrasound facilitate its in-line implementation in the industry. In the meat sector, there are extensive references to the use of ultrasonics for non-destructive testing, which could be explained by considering the significant economic importance of this sector and the lack of reliable non-destructive alternatives for in-line implementation. Thus, ultrasound has been used to determine fat and/or water content in meat-based products (sobrassada, sausages) (Benedito et al., 2001; Simal et al., 2003), in *Biceps femoris* muscle from Iberian pork (Niñoles et al., 2011), in green pork hams (de Prados et al., 2015) and in Iberian dry-cured ham slices (Corona, García-Pérez, Mulet, & Benedito, 2013) through ultrasonic velocity measurements. Likewise, ultrasound has been used to estimate the salt content in brined (de Prados et

al., 2015b) and in dry salting (de Prados et al., 2016) *Biceps femoris* and *Longissimus dorsi* pork muscle, as well as in hams (de Prados et al., 2016). Corona, García-Pérez, Santacatalina, Ventanas, & Benedito (2014) also analyzed the crystallization pattern of two types of Iberian pork fat during cooling, finding out that ultrasonic measurements were useful both to differentiate between fats of differing composition and to characterize the textural changes taking place. As regards food textural properties assessed by ultrasound, Nowak, Markowski, & Daszkiewicz (2015) compared the mechanical properties of sausages estimated by means of both a compression test and by acoustic measurements and concluded that they did not significantly differ. Furthermore, ultrasonic velocity has been used to evaluate the texture of a meat-based product (Llull et al., 2002) and the textural changes undergone by high pressure treated vacuum-packed dry-cured ham slices during cold storage (Corona, García-Pérez, Mulet, & Benedito, 2013). Similarly, ultrasound has been applied to detect textural changes both in beef from old livestock (Dwyer, Mullen, Allen, & Buckin, 2001) and under stress conditions (Swatland, 2001),which may be used as quality indicators of beef meat. In this sense, rapid and non-destructive ultrasound measurements could be useful to assess pastiness, permitting the inline separation of defective from non-defective dry-cured hams. In this way, hams with a high degree of pastiness would not be placed on the market, ensuring a homogeneous and high quality product. Moreover, once defective hams were detected and separated, subsequent corrective treatments could also be applied.

Considering what is mentioned above, the objective of this study was to gain greater knowledge as regards the characterization of ham pastiness from a physicochemical and microstructural point of view, as well as to evaluate the feasibility of using ultrasound to detect pastiness in dry-cured ham.

2. Materials and methods

2.1. Ham elaboration process and sampling procedure

Two hundred hams (pH<5.5 measured in *Semimembranosus* muscle after 24 h postmortem) from Large White and Landrace animal breed crosses were supplied by a commercial slaughterhouse. Initial average weight of hams was 11.9±1.1 kg. In order to induce pastiness of different intensities in hams, a customized elaboration process was conducted. Hams were manually rubbed with the following mixture (g/kg of raw ham): 0.15 of KNO_3, 0.15 of $NaNO_2$, 1.0 of dextrose, 0.5 of ascorbic acid and 10 of NaCl, and then pile salted (3±2 ºC, 85±5% RH) for 4, 6, 8 and 11 days (n=200, 50 hams per salting time). After salting, the superficial salt was removed by using compressed air and afterwards, the hams were brought to post-salting for 45 days (3±2 ºC, 85±5% RH). Once post-salting finished, the hams were subjected to an initial convective drying process (12±2 ºC, 70±5% RH) in order to reduce their weight by 29%. After initial drying, the hams were vacuum-packed and kept at 30 ºC for 30 days trying to induce high proteolysis levels in a large number of hams. Afterwards, the hams were unwrapped and subjected to a second drying process (12±2 ºC, 65±5% RH), which was extended until a final weight loss of 34% was reached. Subsequently, the hams were vacuum-packed and kept at 30 ºC for 30 days. Finally, the unwrapped hams were dried until a final weight loss of 36% was attained. On average, the drying stage lasted approximately 400 days.

Once the elaboration process ended, the femur bone was removed and the aitch bone and the butt end were cut before the cushion part of the ham was excised in order to obtain different slices. Three slices (1.5 mm thick) were used for sensory characterization and one slice (20 mm thick) was employed for physicochemical, microstructural and ultrasonic analyses. The slices were vacuum-packed in individual plastic bags of polyamide/polyethylene (oxygen permeability of 50 cm^3/m^2/24h at 23 ºC

156 and a water permeability of 2.6 g/m^2/24h at 23 ºC and 85% RH, Sacoliva® S.L., Spain)
157 and stored at 4±2 ºC until the analysis was performed.

158 *2.2. Sensory texture analysis*

159 A three-member expert panel, trained following the American Society for Testing and
160 Materials standards (ASTM, 1981), performed the sensory texture analysis. The only
161 textural attribute evaluated in the *Biceps femoris* (BF) muscle was pastiness, which can
162 be defined as a feeling similar to the mouth-coating sensation produced by flour-water
163 paste during the mastication process. The dry-cured ham pastiness level was ranked
164 from score 0 (absence) to 6 (maximum intensity). The pastiness level of the samples
165 was set as the average score of the three experts. Thus, the textural defect of the dry-
166 cured ham was used to classify it into the following sample groups: non-pasty
167 (pastiness level<1), medium-pasty (pastiness level between 1 and 2.5) and highly-
168 pasty (pastiness level>2.5).

169

170 *2.3. Chemical analyses*

171 The pH was measured using a Crison Basic pH meter (Crison Instruments S.A.,
172 Barcelona, Spain). The salt content was analysed using a potentiometric titrator 785
173 DMP Titrino (Metrohm AG, Herisau, Switzerland) following standard methods
174 (ISO1841-2, 1996) and the results were expressed as a percentage of NaCl on a wet
175 basis (w.b.). The moisture content was determined by oven drying to constant weight at
176 103±2 °C following the standard AOAC method, 950.46 (AOAC, 1997). The proteolysis
177 index (PI, %) was calculated as the ratio between non-protein nitrogen and total
178 nitrogen content following the methodology reported by Schivazappa et al. (2002). All
179 the analyses were carried out in triplicate.

180

181 *2.4. Microstructural evaluation*

182 The dry-cured ham microstructure was observed using two microscopic techniques:
183 light microscopy (LM) and transmission electron microscopy (TEM). From slices 1.5
184 mm thick, small sections (5 x 3 mm) were cut from BF muscle with a disposable blade.
185 In order to obtain included sections, the samples were fixed with a 25 g/L
186 glutaraldehyde solution (0.025 M phosphate buffer, pH 6.8, at 4 ºC, 24 h), postfixed
187 with a 20 g/L OsO_4 solution (1.5 h), dehydrated using a graded acetone series (300,
188 500, 700 and 1000 g/kg), contrasted in 40 g/L uranyl acetate dissolved in acetone and
189 embedded in epoxy resin (Durcupan, Sigma–Aldrich, St. Louis, MO, USA). The
190 samples were cut using a Reichert Jung ultramicrotome (Leica Mycrosystems, Wetzlar,
191 Germany). Thin sections (1.5 µm) were stained with 2 g/L toluidine blue and examined
192 in a Nikon Eclipse E800 light microscope (Nikon, Tokyo, Japan). Ultrathin sections (0.5
193 µm) were stained with 40 g/L lead citrate and observed in a PhilipsEM400 (Philips,
194 Eindhoven, Holland) transmission electronic microscope at 80 kV.
195
196 *2.5. Instrumental texture analyses*
197 From dry-cured ham slices, 5 parallelepipeds of BF muscle were carved (20 mm length
198 x 20 mm width x 15 mm height). The textural properties of dry-cured ham
199 parallelepipeds were measured using a TA-XT2 texturometer (SMS, Godalming, UK)
200 provided with a load cell of 50 kg. Stress-relaxation tests were carried out at a constant
201 temperature (4±2 ºC) using a flat 75 mm diameter aluminum plunger (SMS P/75). The
202 samples were compressed to 25% of their initial height perpendicularly to the fiber
203 bundle direction at a crosshead speed of 1 mm/s and afterwards, the probe was held
204 for 90 s to monitor relaxation. The experimental data were recorded and processed
205 with Exponent Lite 6.1.4.0 software (SMS, Godalming, UK). Thus, hardness was
206 computed from the force versus time profiles as the maximum force achieved during
207 compression (F_0) and the level of force decay Y_t logged during relaxation was
208 calculated as follows:

209 $$Y_t = \frac{F_0 - F_t}{F_0} \quad (2)$$

210 where F_0 is the maximum force during compression (N) and F_t is the force recorded
211 after t seconds of relaxation. Y_t was calculated at t=2 s of the relaxation period and at
212 the end of the stress-relaxation test (t=90 s).

213

214 *2.6. Ultrasonic experimental set-up and measurements*

215 Ultrasonic measurements were taken in BF muscle. As shown in Figure 1A, circular
216 measuring points (matching transducer diameter of 1'') were marked on the plastic bag
217 in order to cover the maximum surface of the BF.

218 A custom fully automatic ultrasonic prototype was designed and built by the ASPA
219 research Group of the Universitat Politècnica de València in order to characterize the
220 dry-cured ham slices. The system is made up of seven main elements, as shown in
221 Figure 1B, and can be operated in both pulse-echo and through-transmission ultrasonic
222 measurement modes. In this study, ultrasonic measurements were taken in through-
223 transmission mode using a pair of aligned narrow-band transducers (1 MHz, 1''
224 diameter, A314S model, Panametrics, Waltham, MA, USA). For that purpose, the
225 receiver transducer (Figure 1B, 3) was embedded in the base of the measurement
226 platform, while the emitter (Figure 1B, 2) was attached to the edge of a rod slide
227 electric actuator moved by a step motor (LEY 16RB model, SMC, Tokyo, Japan)
228 (Figure 1B, 1) and controlled (LECP6N model, SMC, Tokyo, Japan) (Figure 1B, 7) and
229 operated under supervision using a computer (Figure 1B, 6).
230 The slice of ham was placed over the receiver transducer and the emitter was moved
231 down by the electric actuator until it reached the slice (initial lowering speed of 250
232 mm/s until a distance between transducers of 40 mm was reached; final lowering
233 speed of 1 mm/s until 17 N of pushing force was exerted on the sample). The pushing
234 force of the transducer on the sample was fixed through the electrical actuator as a

235 threshold to stop the transducer, providing an appropriate sample-transducer coupling
236 and avoiding excessive sample deformation. In addition, tap water was used as
237 coupling material. The electrical actuator was also used to measure the thickness of
238 the slice (±0.01 mm).
239 The pulser-receiver (5058PR model, Panametrics, Waltham, MA, USA) (Figure 1B, 4)
240 working in through-transmission mode (gain 40 dB; excitation voltage (100-400 V) and
241 attenuation (0-40 dB) set depending on the sample requirements) supplied a spike
242 pulse to the emitter transducer (Figure 1B, 2) and also filtered (high pass filter, 1 MHz)
243 and conditioned the electrical signal received from the ultrasonic receiver transducer.
244 Finally, the ultrasonic signal was digitized (sampling frequency 100 Ms/s) by an
245 oscilloscope (USB-5133 model, National Instruments, Austin, USA) (Figure 1B, 5) and
246 sent to the computer for analysis (Figure 1B, 6). An application was developed in
247 LabVIEW^{TM} (National Instruments, Austin, Texas) to integrate the movement of the
248 transducer, the measurement of the sample thickness and the acquisition and
249 recording of the ultrasonic signal.
250 The number of experimental measurement points marked on the BF was between 5
251 and 6 (Figure 1A). An average of 10 signal acquisitions were carried out for each
252 measurement point.
253
254 *2.7. Ultrasonic signal analysis and parameter determination*
255 Figure 2 illustrates a characteristic ultrasonic signal acquired for the dry-cured ham
256 slices using the experimental set-up described in section 2.6. In Figure 2, three
257 wavefront arrivals are observed. The first wavefront arrival corresponds to the direct
258 transit of the ultrasonic signal from the emitter to the receiver transducer and is voltage-
259 saturated (signal is trimmed above ±1.1 V amplitude). The second and third wavefront
260 arrivals (Figure 2) correspond to the two consecutive wave reflections between
261 transducers and are not saturated. Thereby, ultrasonic velocity was measured from the
262 first wavefront arrival, while for the attenuation coefficient, the second and third

wavefronts were considered. Consequently, the time of flight of the ultrasonic signal was computed by using the energy threshold method (upper and lower thresholds 0.1 and -0.1 V, respectively) applied to the first wavefront arrival and considering the system delay (0.7895 μs), as described by de Prados, Fulladosa, et al. (2015). Thus, the ultrasonic velocity (V) was computed as the ratio between the sample thickness and the time of flight. For the attenuation calculation, the analysis was performed in the frequency domain by applying the Fast Fourier Transform (FFT) to the time domain signal. Data in the frequency domain is a complex number consisting of a module and a phase that give rise to a module spectrum (amplitude) and phase spectrum (frequency), respectively. From the frequency domain, the ultrasonic attenuation coefficient (α, Equation 1) was calculated by computing the maximum amplitude of the spectrum corresponding to the second and third wavefront arrivals of energy:

$$\alpha = \frac{Ln\left(\frac{P_3}{P_2}\right)}{2L} \quad (1)$$

where P_3 and P_2 are the maximum amplitudes in the spectrum of the third and second wavefront arrivals of the ultrasonic signal, respectively, and L is the sample thickness. Finally, the average ultrasonic velocity and attenuation coefficient of BF, computed from the 50-60 acquired signals per slice, was correlated to the textural, chemical and sensory parameters of the dry-cured hams.

2.8. Statistical analysis

A one-way analysis of variance (ANOVA) was performed to study the effect of chemical, textural and ultrasonic parameters on the level of pastiness. Subsequently, a linear and polynomial regression was carried out in order to discover a relationship between the level of pastiness and the aforementioned parameters. Eventually, a discriminant analysis was performed to classify the samples into NP, MP or HP levels according to the chemical, textural and ultrasonic parameters measured. All the

289 statistical analyses were carried out using Statgraphics Centurion XVI (Statpoint
290 Technologies Inc., Warrenton, VA, USA)
291

3. Results and discussion

3.1. Levels of pastiness

Hams were classified into three groups according to their level of sensory pastiness. The average pastiness of the non-pasty (NP) group (pastiness level<1) was 0.3±0.2 and it comprised 110 samples. 50 samples were classified into the medium-pasty (MP) group (pastiness level between 1 and 2.5) with an average pastiness of 1.7±0.5. The remaining 40 hams belonged to the highly-pasty (HP) group (pastiness level>2.5), reaching an average pastiness of 3.6±0.3. These results confirmed that 45% of the hams obtained using the ham elaboration process described in section 2.1 had a measurable level of pastiness. Further sections will address the characterization of pastiness by means of chemical, textural, microscopy and ultrasonic techniques.

3.2. Chemical characterization of pastiness

Earlier literature suggested that salt and water contents had a strong influence on the incidence, not only of pastiness, but also of the so-called soft textures in commercial dry-cured hams. Thereby, Gou, Morales, Serra, Guàrdia, & Arnau (2008) reported that defective hams with soft textures presented a lower amount of salt compared to the average quantity found in commercial ones. In a similar way, Serra, Ruiz-Ramírez, Arnau, & Gou (2005) affirmed that an excessive moisture content led to softer textures in hams. High salt contents protect the ham from the action of proteolytic enzymes responsible for the intense proteolysis found in pasty dry-cured hams (Pérez-Santaescolástica et al., 2018). This explains why the intensity of pastiness in standard commercial hams increases as does the probability of the incidence of the defect in the case of low salt contents. In the same way, high water contents promote proteolytic activity, which also fosters the appearance of and increase in pastiness.

The processing conditions used in this study (section 2.1) permitted the removal of the influence of both the salt and water contents on pastiness. The salt content increased

along with the salting time, this being 3.7±0.4, 4.6±0.5, 5.1±0.5 and 5.6±0.7; w.b.% for 4, 6, 8 and 11 salting days, respectively. However, when the hams were divided according to their pastiness intensity (NP, MP and HP), the three groups presented a similar average salt content (NP: 4.8±0.1, MP: 4.8±0.2, HP: 4.7±0.2; w.b.%). A linear regression demonstrated that there was no statistically significant ($p>0.05$) relationship between ham pastiness and salt content ($r=0.0046$). Analogous results were found for the moisture content, where the three groups of ham pastiness presented similar average moisture contents (NP: 58.9±0.1, MP: 58.7±0.2, HP: 59.0±0.2; w.b.%) and the correlation between pastiness and moisture was not statistically significant ($p>0.05$). These results confirmed that, even considering that both salt and moisture content have an intrinsic influence on the appearance and intensity of pastiness, the defect can also appear eventually in hams with a high salt and low moisture content; this is a highly relevant finding, since in earlier literature dealing with pastiness, the salt content always appeared as a significant factor (García-Rey et al., 2004; Morales et al., 2007b). This confirms that the interaction of the processing conditions (excessively high temperatures and vacuum-packaging), may induce the development of pastiness, even at high salt contents.

The proteolysis index (PI) was used for the characterization of pastiness, since a defective texture in ham has been associated with significant proteolysis if compared to ham with a standard texture (Garcia-Garrido et al., 1999; Gou et al., 2008; Ruiz-Ramírez et al., 2006). The range of PI identified for the three groups of pastiness was quite narrow since the values ranged from 28 to 44%. These PI figures were moderately higher than the values reported by Harkouss et al. (2015) studying Bayonne dry-cured hams (25±1%). The statistical analysis carried out for the PI percentage indicated that there exist significant differences ($p<0.05$) between groups of pastiness (Table 1), the PI increasing linearly with the intensity of the defect. Thus, the greater the degree of pastiness, the higher the PI; the MP and HP samples exhibited a PI that was nearly 6.6 and 16.8% greater, respectively, than the NP ones. Virgili et al.

347 (1995) stated that the textural defect was a consequence of abnormal protein cleavage
348 or uncontrolled proteinase activity during ham processing. Figure 3 shows the
349 relationship between PI and pastiness for every ham elaborated in this study, which
350 follows a significant ($p<0.05$) linear upward trend. A high degree of variability was
351 found, especially in NP hams (pastiness level<1) where PI ranged from 28 to 37%. The
352 special ham elaboration process carried out in the present study could explain this fact.
353 Garcia-Garrido et al. (1999) found a good correlation ($r=0.876$) between pastiness
354 (sensory assessed) and non-protein nitrogen in dry-cured ham BF muscle, which is a
355 factor directly related to the PI ratio. The close correlation found in that study could be
356 explained by considering that those authors used commercial hams, where salt and
357 moisture contents are directly linked to proteolysis, reducing the experimental
358 variability. Previous studies have related the PI to the salt content. Thus, Morales,
359 Serra, et al. (2007) observed that dry-cured ham with different salting levels (1, 2, 4%)
360 led to different PI (19.3, 17.8, 16.7%, respectively). However, the PI and the salt
361 content of the hams in this study were not significantly ($p>0.05$) related ($r=0.02$), which
362 again could be due to the special elaboration process, where pastiness was forced by
363 adding processing stages where water was not allowed to leave the packaged samples
364 and temperature was kept at 30 ºC.

365

366 *3.3. Textural characterization of pastiness*

367 The texture of dry-cured hams was characterized by an instrumental stress-relaxation
368 test, as described in section 2.5. The statistical analysis showed significant ($p<0.05$)
369 differences between the hardness of the different groups of pastiness. The samples
370 became softer as the pastiness increased; those dry-cured hams with no textural
371 defects had the highest hardness values (Table 1). Thus, the average hardness of HP
372 ham was 5.4±1.1 N, nearly 68% softer than NP samples; in MP samples, meanwhile,
373 the hardness was 9.5±1.0 N, 43% softer than NP hams. The softer texture of dry-cured

374 ham, classified as HP and MP samples, could be explained by an excessive proteolytic
375 denaturation emerging from the customized elaboration process. In earlier literature,
376 the dry-cured ham texture has been related to the salt content, since salt can affect the
377 proteolytic process and the myofibril structure. Thus, Gou et al. (2008) stated that BF
378 muscle from hams salted for 14 days had a lower degree of pastiness and were harder
379 compared to hams salted for 6 days. In their study, Morales, Serra, et al. (2007) also
380 found that the dry-cured ham with the highest salt content (avg. 4%) exhibited the
381 highest degree of hardness and the lowest PI. However, in the present study, the
382 samples had a similar salt content but a statistically ($p<0.05$) different texture in every
383 group of pastiness. The influence of the level of pastiness on the sample hardness is
384 depicted in Figure 4A, which shows how the hardness decreased as the samples grew
385 pastier. As can be observed, a high degree of variability in terms of hardness was
386 found for non-defective samples (pastiness level<1). The best mathematical
387 description of experimental data was found for a polynomial equation (order 3) which
388 explained 57% of the experimental variability.

389 As for the relaxation properties, both Y_2 and Y_{90} increased as the degree of pastiness
390 rose (Table 1), showing significant differences ($p<0.05$) for the three groups of
391 pastiness. As an increase in force decay is linked to a loss in muscle elasticity, higher
392 Y_2 and Y_{90} values indicate lower elasticity. Another study carried out on dry-cured ham
393 with defective texture presented slightly lower values of Y_2 (0.360) and higher values of
394 Y_{90} (0.734) (Morales et al., 2007a) compared to the ones obtained in the present study.
395 The relative increase in Y_2 for the samples with medium and high pastiness levels
396 compared to the NP pastiness group was 10 and 16.7%, respectively. In the case of
397 Y_{90}, however, the relative increase with respect to the MP and HP samples was merely
398 4.7 and 6.6%, respectively, which points to the fact that Y_2 is a more useful parameter
399 with which to discriminate between pastiness levels than Y_{90}.

400 The linear relationship between both Y_2 (Figure 4B) and Y_{90} (data not shown) and
401 pastiness explained 46 and 35% of the experimental variability, respectively, which

402 represents a moderately strong correlation between both variables. In this sense,
403 similar results were obtained by Gou et al. (2008) who found an analogous tendency
404 between pastiness and instrumental texture parameters in the BF muscle of dry-cured
405 ham: the higher the degree of pastiness, the lower the hardness level and the higher
406 the Y_2 and Y_{90}. However, literature has supplied no quantitative relationship between
407 pastiness and the textural parameters.

408

409 *3.4. Microstructural characterization of pastiness*

410 Dry-cured ham muscle tissue was observed by LM and TEM. Figure 5 shows LM
411 (Figure 5, 1-6) and TEM (Figure 5, 7-9) images of BF muscle tissue from dry-cured
412 ham with different levels of pastiness. Inside the cell, gaps can be observed brought
413 about by the processing undergone by the muscle when transformed into ham. Most of
414 the muscle cells are still composed of structured and packed myofibrils, enclosed by
415 sarcolemma membrane (Figure 5, 2). In general, connective tissue that surrounds
416 muscle cells can be seen to be slightly degraded, especially sarcolemma membrane,
417 but the typical cell structure is still observed (Figure 5, 1). In contrast, muscle tissue
418 with a medium level of pastiness (Figure 5, 3-4) is not uniformly stained and significant
419 gaps appear. Some cells are degraded due to myofibril disintegration (Figure 5, 4).
420 Both endomysium and perimysium connective tissues are demoted (Figure 5, 3).
421 Furthermore, the sarcolemma membrane appears degraded in some parts, giving rise
422 to gaps between the myofibrils and the sarcolemma. Finally, in samples with a high
423 level of pastiness (Figure 5, 5-6) muscle tissue does not have structural integrity. In
424 many parts, the sarcolemma membrane and connective tissue are broken down and
425 even disappear. Muscle cells are largely degraded, merged and do not show structural
426 limits. At a microstructural level, pastiness is generally observed as a high degree of
427 disintegration in the tissue, especially in the cell membranes.

As regards the ultrastructure, and as previously observed by Larrea et al. (2007), standard dry-cured ham (Figure 5, 7) presents an ultrastructure where the proteolysis originating during the curing process may be appreciated (Benedini et al., 2012). Myofibrils and the filaments they are composed of are slightly degraded with no continuity in some areas, which gives rise to small empty spaces or gaps inside the myofibrils. Structural elements of the myofibril can be partially observed. Thus, the H-zone and “A” band can still be distinguished in many parts of the muscle. Almost the entire length of the sarcomere seems to be occupied by the “A” band, with the “I” band remaining hidden. Z-disks, which mark the length of the sarcomere, can be clearly distinguished, although they are no longer aligned. Furthermore, some structural elements that can be easily appreciated in raw muscle, such as the “I” band (Larrea et al., 2007), disappear in cured muscle probably due to a marked proteolytic activity. Intermyofibrillar protein connections (costamere) that join the myofibrils are degraded, bringing about remarkable gaps between myofibrils in many zones. As a result, neighboring myofibrils become compacted, losing their structural identity.

In general, BF muscle from dry-cured ham samples with medium and high levels of pastiness (Figure 5, 8-9) exhibits a high degree of damage compared to dry-cured ham without pastiness; this increases as the level of pastiness rises. In most cases, myofibrillar structural elements in muscle with medium and high levels of pastiness are repeatedly degraded and occasionally disappear, showing a merged protein structure. This indicates a high degree of proteolysis in pasty samples, steeper in samples with high levels of pastiness. Solute accumulation from the proteolysis can be appreciated in the gaps formed as a result of tissue disintegration. Z-disks are considerably degraded, surrounded by gaps, and disappear in many areas of samples with medium levels of pastiness; in samples with a high level of pastiness, there are no Z-disks in most of the tissue. The rest of the myofibrillar structural elements that can be observed in NP dry-cured ham, such as H-zone and costamere structures, cannot be appreciated in pasty samples, regardless of the level of pastiness. In addition, the

456 development of pastiness seems to be characterized by an intense tissue degradation,
457 the merging of myofibril structures and the appearance of large gaps, where material
458 originating from an intense proteolysis of myofibrillar structural components is
459 accumulated.
460 It could be concluded that, in pasty hams, proteolysis led to important structural
461 changes in the muscle cells, such as myofibril degradation and gap formation, which
462 caused ham textural changes (decrease in hardness and elasticity), as observed in
463 section 3.3.
464

465 *3.5. Ultrasonic characterization of pastiness*

466 An ultrasonic non-destructive analysis was carried out in dry-cured ham BF muscle
467 using the through-transmission mode. Two ultrasonic parameters were computed:
468 velocity and attenuation. The ultrasonic velocity obtained for NP samples was 1723±2
469 m/s, which concurred with earlier findings for other dry-cured ham parts. In this sense,
470 the ultrasonic velocity in Iberian dry-cured ham slices from the butt end and fore
471 cushion was 1732±2 and 1765±2 m/s, respectively (Corona et al., 2013). The
472 ultrasonic velocity was significantly ($p<0.05$) related to the moisture ($r=0.69$) and salt
473 contents (0.79), as illustrated in Figure 6 and already reported in literature. Thus, when
474 working on raw hams, de Prados et al. (2015a) found that the higher the moisture
475 content, the greater the ultrasonic velocity ($r=0.95$). As for the salt content, earlier
476 literature reported that ultrasound velocity was closely related with the salt content in
477 dry-cured ham ($r=0.730$) (Fulladosa et al., 2015). Both the moisture and salt content
478 could be related to ultrasonic velocity since the loss of water and the gain of soluble
479 solids increased the bulk modulus and hence the velocity of the ultrasound. Likewise,
480 ultrasonic velocity has been used previously to evaluate textural properties. As an
481 example, Corona et al. (2013) found that an increase in the hardness of lean and fatty
482 tissue led to a rise in ultrasonic velocity. However, in the present study, there were
483 found to be no significant ($p>0.05$) differences between the velocity figures and the

484 textural parameters. Thereby, as illustrated in Table 1, the different groups of pastiness
485 showed similar ultrasonic velocities, which indicates that this parameter was not
486 capable of characterizing this defect.

487 As for the ultrasonic attenuation coefficient, an average figure of 43±1 Np/m was found
488 in NP samples (Table 1). To our knowledge, no previous attenuation coefficient data
489 have been reported for dry-cured ham. For raw meat, Koch et al. (2011) computed a
490 value of 12±3 Np/m, for porcine *Longissimus* muscle at 24 h *post mortem*. The greater
491 attenuation value found for dry-cured ham could be due to the lower water content held
492 in the samples of the present study. Neither the moisture nor the salt content were
493 found to have any influence on the attenuation coefficient. However, this parameter
494 was significantly ($p<0.05$) affected by the textural attributes, such as hardness,
495 relaxation capacity and pastiness. The evaluation of changes in meat texture through
496 ultrasonic attenuation has already been reported in the literature. Ayadi, Culioli, &
497 Abouelkaram (2007) established a good relationship ($r=-0.81$) between attenuation and
498 stress at 20% deformation during the ageing period of BF muscle from beef cattle:
499 attenuation decreased due to the fact that during the onset of *rigor-mortis,* the rigidity of
500 meat increases. In this study, the analysis of variance of the ultrasonic attenuation
501 coefficient revealed significant differences ($p<0.05$) between the different groups of
502 pastiness (Table 1).Thus, the highest attenuation coefficient was found in HP samples
503 (48±2 Np/m). As regards NP ham, the greatest relative increase in the attenuation
504 coefficient was found in the HP group (11.8%), which was more than twice that of the
505 MP samples (5.3%). The fact that attenuation increased as the level of pastiness rose
506 could be explained by the greater energy loss of the ultrasonic wave when passing
507 through a highly viscous medium (HP sample) compared to a normal one (NP sample).
508 Overall, relative changes in the attenuation coefficient regarding NP samples (MP:
509 5.3%; HP: 11.8%) were similar to the rest of the parameters measured (PI, Y_2, and Y_{90})
510 (Table 1). However, bigger changes were found for hardness, reaching percentages of
511 43.1 and 67.7% for MP and HP samples compared to NP ones, respectively. This

indicates that the hardness parameter seems the most sensitive of the ones used in this study to any modification caused by pastiness.

Finally, a discriminant analysis was carried out with the parameters that showed statistical significance ($p<0.05$) between the three groups of pastiness. Thus, the classification functions obtained with PI, hardness, Y_2, Y_{90} and attenuation coefficient parameters were able to classify 72% of the ham samples in the correct group of pastiness.

Based on the results obtained, using ultrasound technology to measure the ultrasonic attenuation coefficient could be a useful means of performing the non-destructive characterization of pastiness in dry-cured ham and, thereby, may help to distinguish between samples with different levels of pastiness.

4. Conclusions

Pastiness was developed in dry-cured ham over a wide range of salt and moisture contents. This reveals that, despite the marked influence of these factors on the development and intensity of pastiness, this defect could eventually appear in samples of high salt and low moisture contents. From the microstructural and ultrastructural study, it could be concluded that, due to the high proteolysis, pasty ham loses its structure, leading to a protein gel wherein the higher the level of pastiness, the greater the structural degradation. These changes in the dry-cured ham structure brought about softer textures and higher relaxation capacities compared to dry-cured ham without pastiness. Non-destructive ultrasonic measurements revealed that the more intense the level of pastiness, the greater the ultrasonic attenuation coefficient. In this sense, ultrasound could be a useful means of performing the non-destructive detection of commercial pasty dry-cured ham with different intensities of pastiness.

Acknowledgements

The authors acknowledge the financial support from the “Spanish Ministerio de Economía y Competitividad (MINECO), Instituto Nacional de Investigación y Tecnología Agraria y Alimentaria (INIA)” in Spain, the European Regional Development Fund (ERDF 2014-2020) (Project RTA2013-00030-C03-02) and the PhD grant of M. Contreras from Universitat Politècnica de València.

References

AOAC, 1997. Official method 950.46, Official Methods of Analysis (16th ed.). Washington, USA: Association of Official Analytical Chemists.

ASTM STP 758, 1981. American Society for Testing and Materials. Guidelines for the selection and training of sensory panel members.

Ayadi, A., Culioli, J., Abouelkaram, S., 2007. Sonoelasticity to monitor mechanical changes during rigor and ageing. Meat Sci. 76, 321–326. https://doi.org/10.1016/j.meatsci.2006.11.016

Benedini, R., Parolari, G., Toscani, T., Virgili, R., 2012. Sensory and texture properties of Italian typical dry-cured hams as related to maturation time and salt content. Meat Sci. 90, 431–437. https://doi.org/10.1016/j.meatsci.2011.09.001

Benedito, J., Carcel, J.A., Rossello, C., Mulet, A., 2001. Composition assessment of raw meat mixtures using ultrasonics. Meat Sci. 57, 365–370. https://doi.org/10.1016/S0309-1740(00)00113-3

Benedito, J., Carcel, J.A., Sanjuan, N., Mulet, A., 2000. Use of ultrasound to assess Cheddar cheese characteristics. Ultrasonics 38, 727–730. https://doi.org/10.1016/S0041-624X(99)00157-2

Corona, E., García-Pérez, J.V., Ventanas, S., Benedito, J.J., 2014a. Ultrasonic characterization of the fat source and composition of formulated dry-cured meat products. Food Sci. Technol. Int. 20, 275–285. https://doi.org/10.1177/1082013213482915

Corona, E., García-Pérez, J. V., Mulet, A., Benedito, J., 2013. Ultrasonic assessment of textural changes in vacuum packaged sliced Iberian ham induced by high pressure treatment or cold storage. Meat Sci. 95, 389–395. https://doi.org/10.1016/j.meatsci.2013.05.008

Corona, E., García-Pérez, J. V., Santacatalina, J. V., Ventanas, S., Benedito, J.,

2014b. Ultrasonic characterization of pork fat crystallization during cold storage. J. Food Sci. 79. https://doi.org/10.1111/1750-3841.12410

de Prados, M., Fulladosa, E., Gou, P., Muñoz, I., Garcia-Perez, J. V., Benedito, J., 2015a. Non-destructive determination of fat content in green hams using ultrasound and X-rays. Meat Sci. 104, 37–43. https://doi.org/10.1016/j.meatsci.2015.01.015

de Prados, M., Garcia-Perez, J. V., Benedito, J., 2016. Ultrasonic characterization and online monitoring of pork meat dry salting process. Food Control 60, 646–655. https://doi.org/10.1016/j.foodcont.2015.09.009

de Prados, M., García-Pérez, J. V., Benedito, J., 2015b. Non-destructive salt content prediction in brined pork meat using ultrasound technology. J. Food Eng. 154, 39–48. https://doi.org/10.1016/j.jfoodeng.2014.12.024

Desmond, E., 2006. Reducing salt: A challenge for the meat industry. Meat Sci. 74, 188–196. https://doi.org/10.1016/j.meatsci.2006.04.014

Dwyer, C., Mullen, A.M., Allen, P., Buckin, V., 2001. Anisotropy of ultrasonic velocity as a method of tracking postmortem ageing in beef. Proc. 47th ICoMST 4, 250.

Fulladosa, E., Austrich, A., Muñoz, I., Guerrero, L., Benedito, J., Lorenzo, J.M., Gou, P., 2018. Texture characterization of dry-cured ham using multi energy X-ray analysis. Food Control 89, 46–53. https://doi.org/10.1016/j.foodcont.2018.01.020

Fulladosa, E., De Prados, M., García-Perez, J. V., Benedito, J., Muñoz, I., Arnau, J., Gou, P., 2015. X-ray absorptiometry and ultrasound technologies for non-destructive compositional analysis of dry-cured ham. J. Food Eng. 155, 62–68. https://doi.org/10.1016/j.jfoodeng.2015.01.015

Fulladosa, E., Rubio-Celorio, M., Skytte, J.L., Muñoz, I., Picouet, P., 2017. Laser-light backscattering response to water content and proteolysis in dry-cured ham. Food Control 77, 235–242. https://doi.org/10.1016/j.foodcont.2017.02.001

596 Garcia-Garrido, J.A., Quiles-Zafra, R., Tapiador, J., Luque De Castro, M.D., 1999.
597 Sensory and analytical properties of Spanish dry-cured ham of normal and
598 defective texture. Food Chem. 67, 423–427. https://doi.org/10.1016/S0308-
599 8146(99)00144-2

600 García-Rey, R.M., García-Garrido, J.A., Quiles-Zafra, R., Tapiador, J., Luque de
601 Castro, M.D., 2004. Relationship between pH before salting and dry-cured ham
602 quality. Meat Sci. 67, 625–632. https://doi.org/10.1016/j.meatsci.2003.12.013

603 Gou, P., Morales, R., Serra, X., Guàrdia, M.D., Arnau, J., 2008. Effect of a 10-day
604 ageing at 30 ^{o}C on the texture of dry-cured hams processed at temperatures up to
605 18 ^{o}C in relation to raw meat pH and salting time. Meat Sci. 80, 1333–1339.
606 https://doi.org/10.1016/j.meatsci.2008.06.009

607 Harkouss, R., Astruc, T., Lebert, A., Gatellier, P., Loison, O., Safa, H., Portanguen, S.,
608 Parafita, E., Mirade, P.S., 2015. Quantitative study of the relationships among
609 proteolysis, lipid oxidation, structure and texture throughout the dry-cured ham
610 process. Food Chem. 166, 522–530.
611 https://doi.org/10.1016/j.foodchem.2014.06.013

612 Koch, T., Lakshmanan, S., Brand, S., Wicke, M., Raum, K., Mörlein, D., 2011.
613 Ultrasound velocity and attenuation of porcine soft tissues with respect to structure
614 and composition: I. Muscle. Meat Sci. 88, 51–58.
615 https://doi.org/10.1016/j.meatsci.2010.12.002

616 Larrea, V., Pérez-Munuera, I., Hernando, I., Quiles, A., Llorca, E., Lluch, M.A., 2007.
617 Microstructural changes in Teruel dry-cured ham during processing. Meat Sci. 76,
618 574–582. https://doi.org/10.1016/j.meatsci.2007.01.013

619 Llull, P., Simal, S., Benedito, J., Rosselló, C., 2002. Evaluation of textural properties of
620 a meat-based product (sobrassada) using ultrasonic techniques. J. Food Eng. 53,
621 279–285. https://doi.org/10.1016/S0260-8774(01)00166-2

López-Pedrouso, M., Pérez-Santaescolástica, C., Franco, D., Fulladosa, E., Carballo, J., Zapata, C., Lorenzo, J.M., 2018. Comparative proteomic profiling of myofibrillar proteins in dry-cured ham with different proteolysis indices and adhesiveness. Food Chem. 244, 238–245. https://doi.org/10.1016/j.foodchem.2017.10.068

Morales, R., Guerrero, L., Serra, X., Gou, P., 2007a. Instrumental evaluation of defective texture in dry-cured hams. Meat Sci. 76, 536–542. https://doi.org/10.1016/j.meatsci.2007.01.009

Morales, R., Serra, X., Guerrero, L., Gou, P., 2007b. Softness in dry-cured porcine biceps femoris muscles in relation to meat quality characteristics and processing conditions. Meat Sci. 77, 662–669. https://doi.org/10.1016/j.meatsci.2007.05.020

Niñoles, L., Mulet, A., Ventanas, S., Benedito, J., 2011. Ultrasonic characterisation of B. femoris from Iberian pigs of different genetics and feeding systems. Meat Sci. 89, 174–180. https://doi.org/10.1016/j.meatsci.2011.04.014

Nowak, K.W., Markowski, M., Daszkiewicz, T., 2015. Ultrasonic determination of mechanical properties of meat products. J. Food Eng. 147, 49–55. https://doi.org/10.1016/j.jfoodeng.2014.09.024

Parolari, G., Virgili, R., Schivazappa, C., 1994. Relationship between cathepsin B activity and compositional parameters in dry-cured hams of normal and defective texture. Meat Sci. 38, 117–122.

Pérez-Santaescolástica, C., Carballo, J., Fulladosa, E., Garcia-Perez, J. V., Benedito, J., Lorenzo, J.M., 2018. Effect of proteolysis index level on instrumental adhesiveness, free amino acids content and volatile compounds profile of dry-cured ham. Food Res. Int. 107, 559–566. https://doi.org/10.1016/j.foodres.2018.03.001

Ruiz-Ramírez, J., Arnau, J., Serra, X., Gou, P., 2006. Effect of pH24, NaCl content and proteolysis index on the relationship between water content and texture

parameters in biceps femoris and semimembranosus muscles in dry-cured ham. Meat Sci. 72, 185–194. https://doi.org/10.1016/j.meatsci.2005.06.016

Schivazappa, C., Degni, M., Nanni Costa, L., Russo, V., Buttazzoni, L., Virgili, R., 2002. Analysis of raw meat to predict proteolysis in Parma ham. Meat Sci. 60, 77–83. https://doi.org/10.1016/S0309-1740(01)00109-7

Serra, X., Ruiz-Ramírez, J., Arnau, J., Gou, P., 2005. Texture parameters of dry-cured ham m. biceps femoris samples dried at different levels as a function of water activity and water content. Meat Sci. 69, 249–254. https://doi.org/10.1016/j.meatsci.2004.07.004

Simal, S., Benedito, J., Clemente, G., Femenia, A., Rosselló, C., 2003. Ultrasonic determination of the composition of a meat-based product. J. Food Eng. 58, 253–257. https://doi.org/10.1016/S0260-8774(02)00375-8

Swatland, H.J., 2001. Elastic deformation in probe measurements on beef carcasses. J. Muscle Foods 12, 97–105.

Virgili, R., Parolari, G., Schivazappa, C., Bordini, C.S., Borri, M., 1995. Sensory and Texture Quality of Dry-Cured Ham as Affected by Endogenous Cathepsin B Activity and Muscle Composition. J. Food Sci. 60, 1183–1186. https://doi.org/10.1111/j.1365-2621.1995.tb04551.x

667 **Figures and table captions**

668 Figure 1. A: Slice of deboned dry-cured ham. The three main muscles are shown:
669 *Biceps femoris* (BF), *Semitendinosus* (ST) and *Semimembranosus* (SM). Circular
670 measurement points for ultrasonic analysis were marked on BF muscle. B: Diagram of
671 the ultrasonic experimental set-up.

672 Figure 2. Ultrasonic signal obtained in the through-transmission mode. The first
673 wavefront corresponds to the direct transit of the ultrasonic signal from the emitter to
674 the receiver transducer. Second and third wavefronts correspond to the two
675 consecutive wave reflections between transducers.

676 Figure 3. Relationship between pastiness and proteolysis index (PI) in slices of dry-
677 cured ham.

678 Figure 4. A: Relationship between pastiness and hardness in slices of dry-cured ham.
679 B: Relationship between pastiness and the force decay textural parameter measured at
680 2 s (Y_2) in slices of dry-cured ham.

681 Figure 5. Light microscopy (1-6) and transmission electron microscopy (7-9)
682 micrographs of *Biceps femoris* muscle tissue from dry-cured ham with different levels
683 of pastiness (20x: 1, 3, 5; 60x: 2, 4, 6; 1200x: 7, 8, 9). C: Costamere; E: Endomysium;
684 G: Gap; M: Myofibril; P: Perimysium; S: Sarcomere; SA: Sarcolemma; SP: Intracelullar
685 Space; Z: Z-line.

686 Figure 6. Relationship between ultrasonic velocity and moisture (A) and salt content (B)
687 in slices of dry-cured ham.

688 Table 1. Average (±LSD intervals/2) of salt and moisture content, proteolysis index (PI),
689 hardness, force decay at 2 and 90 s (Y_2 and Y_{90}), ultrasonic velocity (V) and ultrasonic
690 attenuation coefficient (α) for dry-cured hams grouped into 3 groups of pastiness.

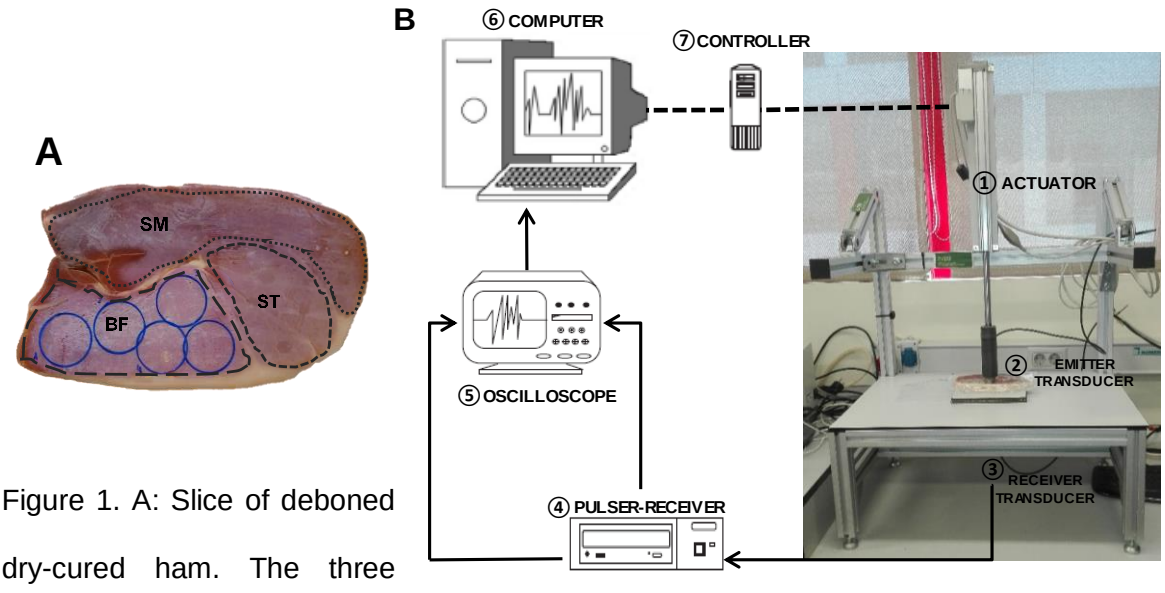

Figure 1. A: Slice of deboned dry-cured ham. The three main muscles are shown: *Biceps femoris* (BF), *Semitendinosus* (ST) and *Semimembranosus* (SM). Circular measurement points for ultrasonic analysis were marked on BF muscle. B: Diagram of the ultrasonic experimental set-up.

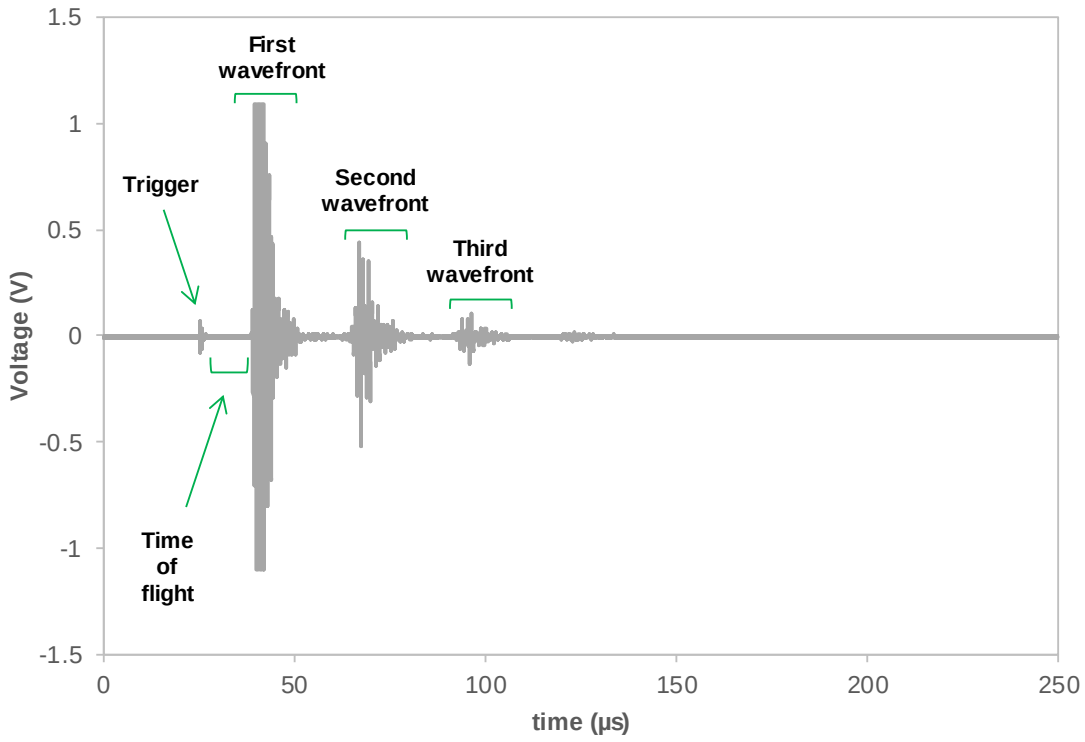

Figure 2. Ultrasonic signal obtained in the through-transmission mode. The first wavefront corresponds to the direct transit of the ultrasonic signal from the emitter to the receiver transducer. Second and third wavefronts correspond to the two consecutive wave reflections between transducers.

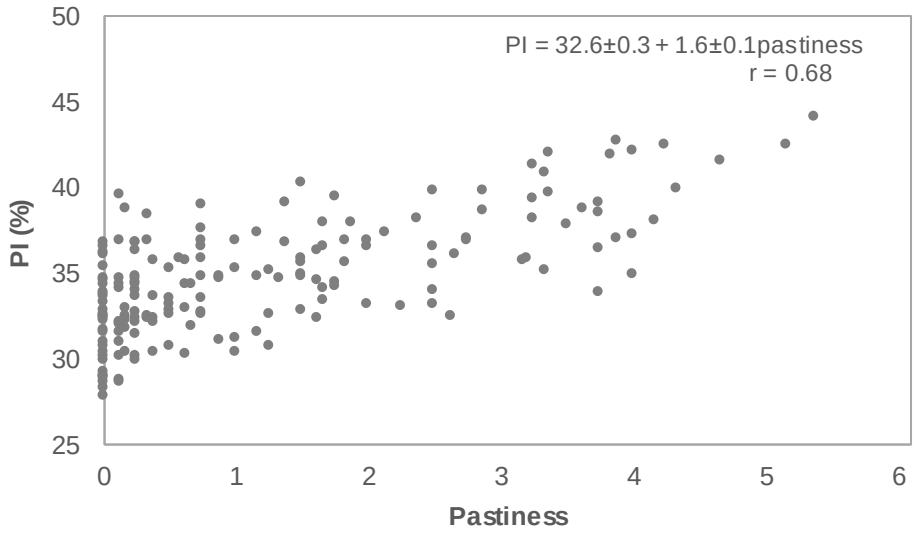

Figure 3. Relationship between pastiness and proteolysis index (PI) in slices of dry-cured ham.

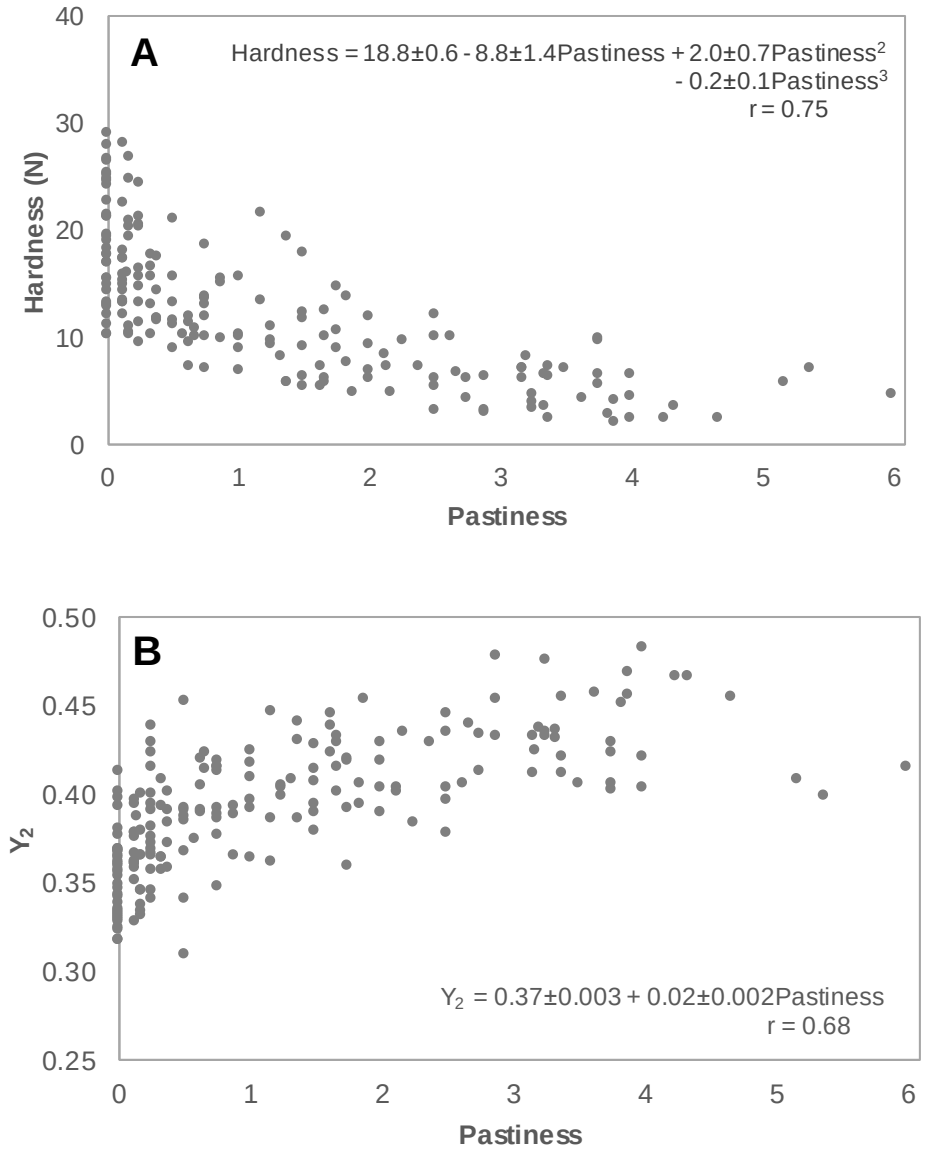

Figure 4. A: Relationship between pastiness and hardness in slices of dry-cured ham. B: Relationship between pastiness and the force decay textural parameter measured at 2 s (Y_2) in slices of dry-cured ham.

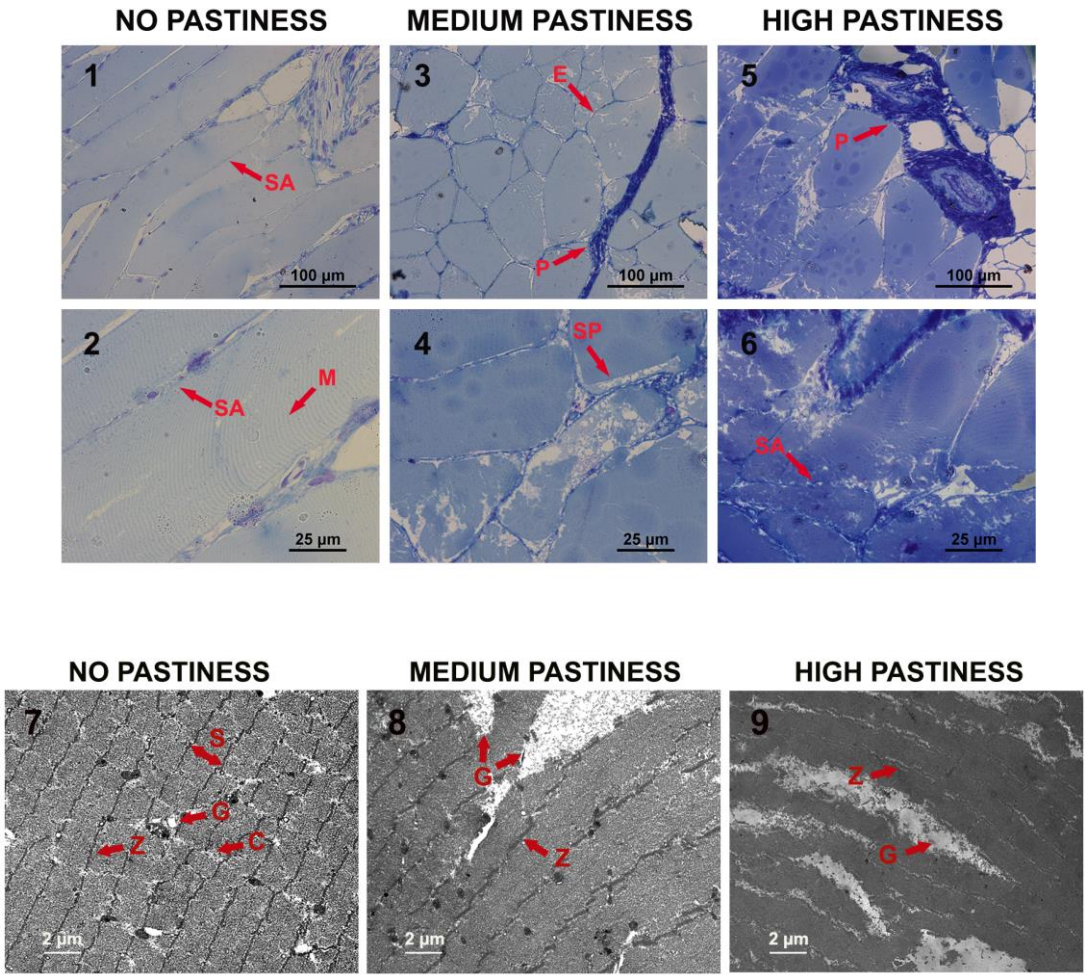

Figure 5. Light microscopy (1-6) and transmission electron microscopy (7-9) micrographs of *Biceps femoris* muscle tissue from dry-cured ham with different levels of pastiness (20x: 1, 3, 5; 60x: 2, 4, 6; 1200x: 7, 8, 9). C: Costamere; E: Endomysium; G: Gap; M: Myofibril; P: Perimysium; S: Sarcomere; SA: Sarcolemma; SP: Intracelullar Space; Z: Z-line.

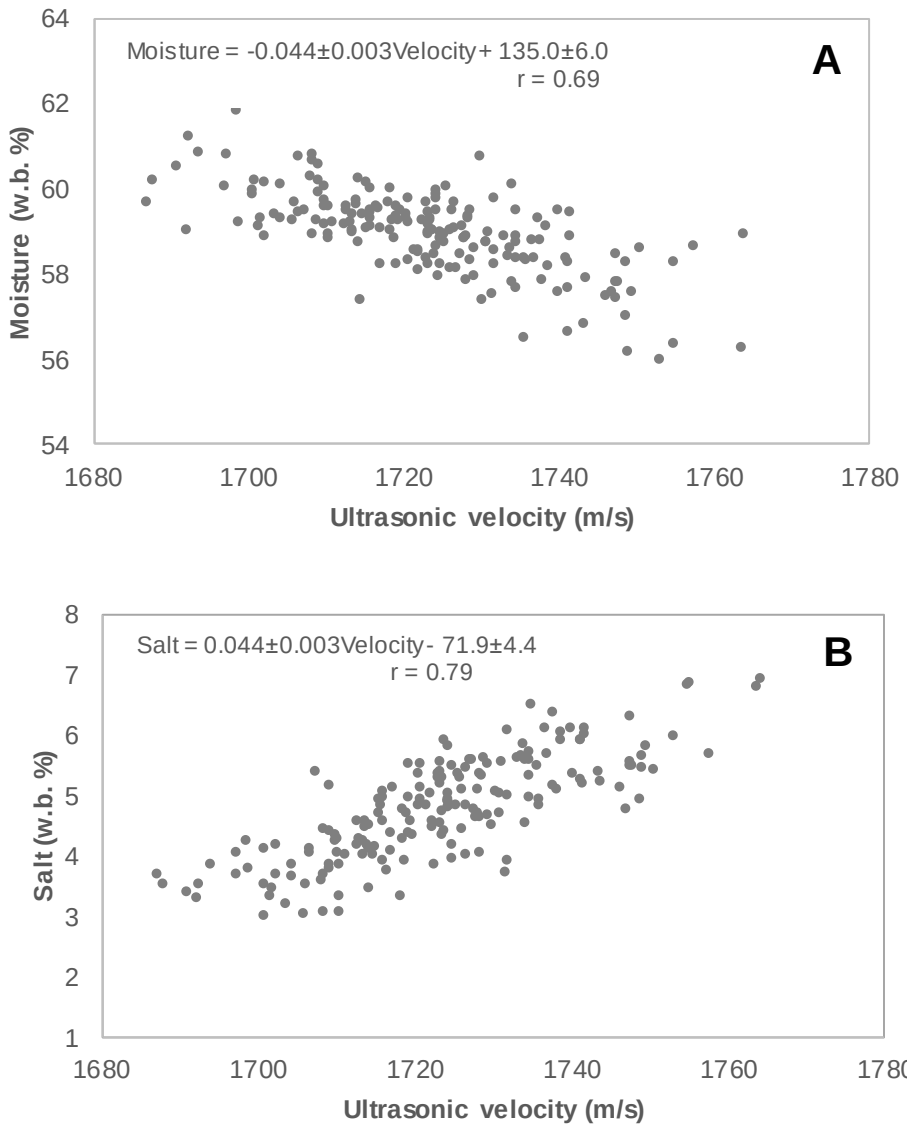

Figure 6. A: Relationship between ultrasonic velocity and moisture (A) and salt content (B) in slices of dry-cured ham.

Table 1. Average (±LSD intervals/2) of salt and moisture content, proteolysis index (PI), hardness, force decay at 2 and 90 s (Y_2 and Y_{90}), ultrasonic velocity (V) and ultrasonic attenuation coefficient (α) for dry-cured hams grouped into 3 groups of pastiness.

	Salt (w.b. %)	Moisture (w.b. %)	PI (%)	Hardness (N)	Y_2	Y_{90}	V (m/s)	α (Np/m)
No pastiness	4.8±0.1^{a}	58.9±0.1^{a}	33.1±0.4^{c}	16.7±0.7^{a}	0.372±0.004^{c}	0.656±0.003^{c}	1723±2^{a}	43.1±0.9^{b}
Medium pastiness	4.8±0.2^{a}	58.7±0.2^{a}	35.3±0.6^{b} (+6.6%)	9.5±1.0^{b} (-43.1%)	0.409±0.005^{b} (+10.0%)	0.687±0.005^{b} (+4.7)	1724±3^{a}	45.4±1.4^{ab} (+5.3%)
High pastiness	4.7±0.2^{a}	59.0±0.2^{a}	38.7±0.6^{a} (+16.8%)	5.4±1.1^{c} (-67.7%)	0.434±0.006^{a} (+16.7%)	0.699±0.005^{a} (+6.6)	1722±3^{a}	48.2±1.5^{a} (+11.8%)

w.b. %: wet basis (kg water/100 kg).

Values in brackets represent the relative increase or decrease (in percentages) for the groups of medium and high levels of pastiness compared to the no pastiness one for each measured parameter.

Superscripts show homogeneous groups established from LSD (Least Significance Difference) intervals ($p<0.05$) for every parameter measured according to the level of pastiness.